Reports

Earthquake Prediction: Variation of Seismic Velocities before the San Francisco Earthquake

Abstract. *A large precursory change in seismic body-wave velocities occurred before the earthquake in San Fernando, California. The discovery that this change is mainly in the* P-*wave velocity clearly relates the effect to the phenomenon of dilatancy in fluid-filled rocks. This interpretation is supported by the time-volume relation obtained by combining the present data with the data from previous studies. The duration of the precursor period is proportional to the square of an effective fault dimension, which indicates that a diffusive or fluid-flow phenomenon controls the time interval between the initiation of dilatancy and the return to a fully saturated condition which is required for rupture.*

The V_P/V_S ratio (*P*-wave velocity/*S*-wave velocity) decreased before the San Fernando earthquake of 9 February 1971 in the same manner as previously reported for experiments in Tadzhik Soviet Socialist Republic (*1–3*) and New York State (*4*). The lead time of the decrease was about 3½ years for this event of magnitude 6.4. The result confirms a previously proposed dependence of anomaly duration on magnitude and extends the relation to a much larger event than has been tested to date. An important characteristic revealed by this study is that most of the velocity variation is in V_P, which in turn causes the large drop in V_P/V_S (10 percent). This result is significant because V_P is much easier to measure than V_S, especially if artificial sources are used. These findings are compatible both qualitatively and quantitatively with the phenomenon of rock dilatancy (an increase of volume due to a change in shape) and its effects on rock strength and fluid saturation. Migration of fluid into the enlarged rock voids is responsible for the time delay between onset of dilatancy and rupture.

Large precursory decreases of the velocity ratio V_P/V_S near the epicentral regions of earthquakes of magnitude 3 to 5 were first reported in the Garm region of Tadzhik (*1–3*). The duration of the decrease was found to lengthen with the magnitude of the event, and V_P/V_S returned to the "normal" value just before the earthquake. The technique was used to plot the time difference between the *S*-wave and *P*-wave arrivals as a function of the *P*-wave arrival time for two or more stations recording the event; this plot is termed a Wadati diagram. The slope of the line through the data, if the transmission medium can be approximated as homogeneous, is a direct measure of the function $(V_P/V_S - 1)$. The same experiment was repeated for an earthquake swarm in the Adirondack region of northern New York State, and it produced consistent results for events ranging in magnitude from 1 to 3 (*4*). It is important to test this technique with larger and potentially more destructive earthquakes.

Two seismic stations in California, PAS (Pasadena) and RVR (Riverside), lie within 120 km of the San Fernando epicentral area and record direct crustal body waves before the arrivals refracted from the Mohorovičić discontinuity (P_n and S_n). The stations are separated by 76 km. Nineteen earthquakes from the time period 1961 to 1970 fit the requirements that they be (i) near the San Fernando epicentral area, (ii) less than 120 km from RVR, (iii) approximately in line with PAS and RVR (in order to minimize uncertainties), and (iv) large enough to give sharp body phases.

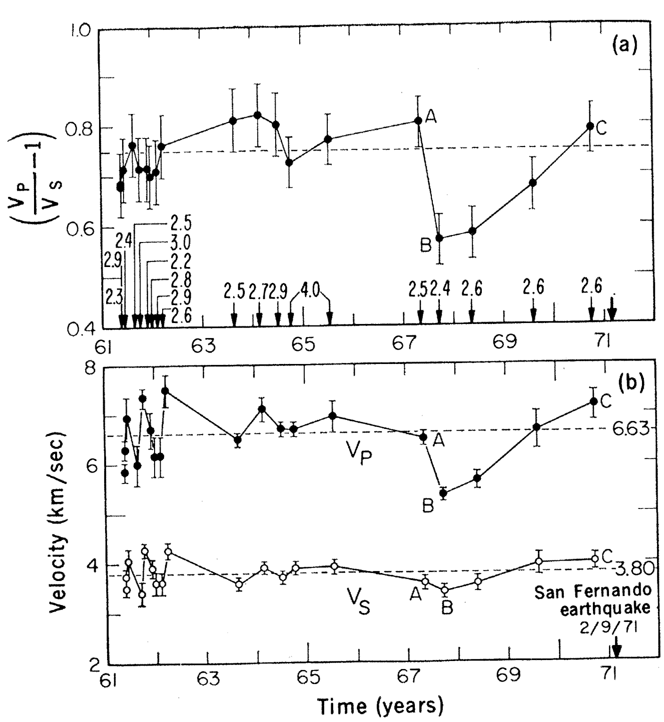

Fig. 1. Variation of (a) $(V_P/V_S - 1)$ and (b) V_P and V_S between PAS and RVR from 1961 through 1970 before the San Fernando earthquake of 9 February 1971. In (a) each point corresponds to an earthquake whose magnitude is shown along the time axis. The maximum estimated error due to an *S*-wave time misreading is shown by the error bars. In (b) the maximum estimated errors due to uncertainties in hypocentral locations and phase times are shown. See the text for an explanation of *A*, *B*, and *C*.

Figure 1a shows the time dependence of $(V_P/V_S - 1)$ during the interval 1961 to 1970. The time of the San Fernando earthquake of 9 February 1971 is indicated with an arrow. The outstanding characteristic of Fig. 1a is the sudden large decrease of $(V_P/V_S - 1)$ in mid-1967 followed by a slower increase to the normal value just before the San Fernando earthquake. The time interval from the onset of the decrease to the earthquake was about 1300 days or 3½ years. The decrease of V_P/V_S in 1967 was 10 percent from its average or normal value of 1.75, which is about the midpoint of the range of values before mid-1967. During this time period, V_P/V_S remained within 4 percent of 1.75.

Figure 1b shows the variation of the apparent velocities V_P and V_S and their respective averages between the stations PAS and RVR. During the precursory interval before the San Fernando earthquake, V_P ranged from -19 percent to $+8$ percent of the average value of 6.63 km/sec. The behavior of V_S is similar but the changes are smaller. Before the earthquake V_S changes from -10 percent to $+5$ percent of its average of 3.80 km/sec in the same sense as V_P, but this change is close to the uncertainties in V_S. Thus, the data clearly indicate that the variation of V_P/V_S is primarily due to large changes of V_P, and not V_S as proposed by Savarensky (*1*) and Aggarwal *et al.* (*4*). This result, clarified here for the first time, is critical for the explanation of the velocity variations that we propose.

We now estimate the possible errors in the observed parameters of Fig. 1a. The *P*-wave and *S*-wave times were read to the nearest 0.1 second on short-period vertical and horizontal seismometers. Onsets of *P* waves are usually clear but it is often difficult to unambiguously pick the *S*-wave onset. The *S*-wave times were read on all available vertical and horizontal short-period seismograms at PAS and RVR (five at PAS and three at RVR), and their averages were taken as the proper values. Figure 2 shows sample recordings both during and before the precursor time. The range of *S*-wave times for an event was 0.5 second or less for all readings from the last event in 1964 through 1970, which covers the precursor time interval. Using the range of 0.5 second for the uncertainty of the *S*-wave readings, we calculate an uncertainty of $(V_P/V_S - 1)$ of ± 0.05, which is shown in Fig. 1a. Some earlier events produced PAS readings that had a range of up to 0.8 second. Use of a 0.8-second range for PAS yields an uncertainty of ± 0.065, which would be applicable to the 1964 and earlier data. The uncertainties of the velocities in Fig. 1b are also dependent on the epicentral locations and their uncertainties, which we estimate to be 12 km. If the two stations are in line with the epicenter, then the effect of epicentral uncertainties on the velocity uncertainties is small. The uncertainties due to assumed epicentral location and time errors as stated above are calculated for each point and shown in Fig. 1b. Although there is no effective control of the depth of the earthquakes, precise locations of many other events in the same area indicate that the hypocenters are limited to depths of 15 km or less (*5*). Even so, if the events were anomalously deep, causing refracted arrivals to be picked first, the only possible effect would be to increase the apparent *P*-wave velocity, the opposite of what is observed. It is apparent that the anomalous behavior of $(V_P/V_S - 1)$ and V_P before the San Fernando earthquake is significant with respect to the estimated uncertainties in the data.

The behavior of V_P/V_S reported here is even more significant when compared with the results of previous experiments. Our average or normal value of V_P/V_S is 1.75, whereas Semenov (*2*) reported 1.77 and Aggarwal *et al.* (*4*) found 1.75. Decreases of V_P/V_S from these norms before earthquakes were 10 percent for the San Fernando event, 6 percent in Tadzhik (*1–3*), and up to 13 percent in New York (*4*). In Tadzhik and New York, the size of the decrease did not appear to be a function of magnitude and was relatively constant.

However, the duration of the decrease, that is, the time from the initial decrease to the occurrence of the earthquake, was found to increase with magnitude (*1–4*). Figure 3 shows the precursor time interval plotted as a function of magnitude for the San Fernando earthquake, the Tadzhik events, and the New York events. The dependence of precursor time interval on magnitude is confirmed by the San Fernando point and extended to a much larger event than investigated to date. If this relationship can be simply extrapolated (as shown by the dashed line) to even larger events, the precursor time interval for a magnitude 7 event would be 8 years, and for a magnitude 8 event, 40 years. However, we cannot be confident of the validity of this extrapolation until many questions are resolved about the nature of the relation between precursor time and magnitude.

All of these phenomena, the nature and especially the amplitude of the velocity changes and their temporal relation to the occurrence and magnitude of earthquakes, agree remarkably well with the known effects of rock dilatancy in fluid-filled, porous media, as described by Frank (*6*), Brace and Martin (*7*), and Nur (*8*). Dilatancy results from increased void, pore, or crack volume. Work is thus done by

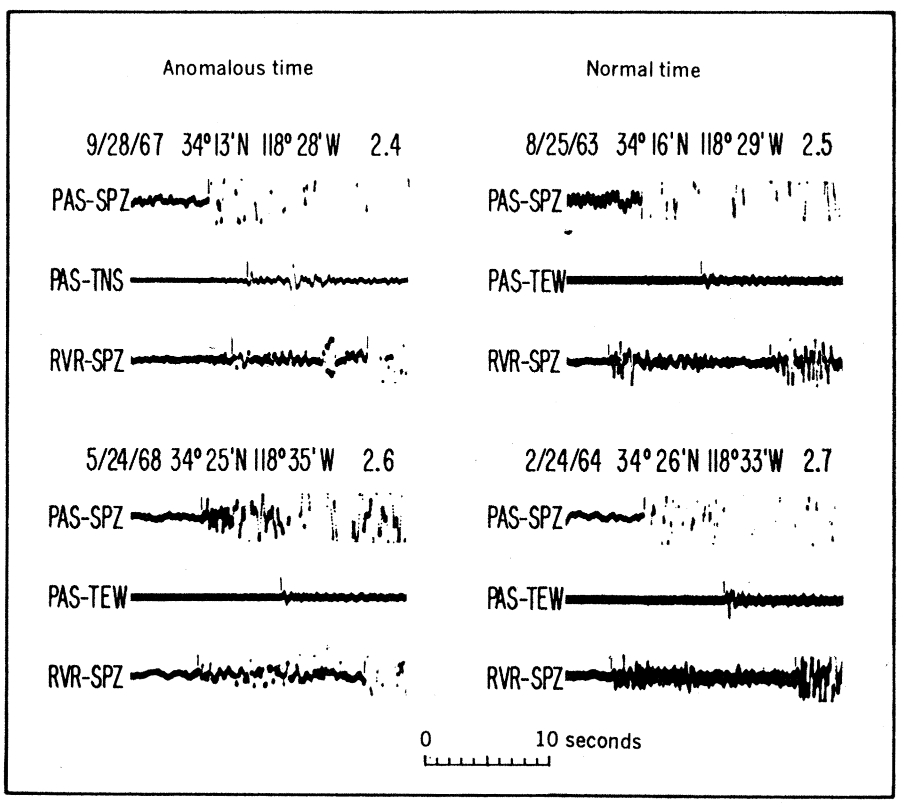

Fig. 2. Examples of PAS and RVR recordings for events during the anomalous time and corresponding events of nearly identical size and location during the normal time. At PAS the abbreviation SPZ (short-period vertical) is used for *P* waves, and TNS or TEW (horizontal torsion) is used for *S* waves; these two records are aligned in time in the figure. At RVR, both *P* and *S* waves are read from SPZ in most cases; the pulses before *P*, especially in the event on 28 September 1967, have the same character as noise elsewhere on the seismogram. For removal of the *P*-wave velocity anomaly (Fig. 1b) the *P*-wave reading at RVR would have to be about 2 seconds earlier in the events on 28 September 1967 and 24 May 1968.

dilatancy against the overall pressure (6). The change in shape is presumably due to shear stresses associated with a regional tectonic strain. If the pores or cracks contain fluid the effect of dilatancy on a saturated rock is to greatly reduce the fluid pore pressure, and if the dilatancy is large enough a state is reached when the pore or crack volume exceeds the fluid volume, which is defined here as undersaturation. Fluid flow eventually returns the rock to its saturated state. But while the fluid pore pressure is below its normal level the fracture strength of the rock is significantly increased, an effect termed dilatancy hardening (6, 7). The reduction in pore pressure can occur rapidly, whereas the return to a saturated condition occurs slowly since it is controlled by fluid flow processes in a permeable medium. If the velocity anomaly depended on the maintenance of new dry cracks in a saturated medium, as Nur (8) suggests, it would be difficult to get a variable anomaly time because the average distance from a dry crack to a wet one would generally remain constant.

The change in *P*-wave velocity takes place when a crack or void in the rock opens enough so that a small amount of vapor is present. This greatly reduces the bulk modulus, causing a large drop in the velocity of *P* waves but little change in that of *S* waves. Laboratory determinations of V_P and V_S in wet and dry crystalline rocks of low porosity under a range of confining pressures have been published by Nur and Simmons (9). Although these are not true measurements of the effect of dilatancy on saturated rocks (dry cracks are not necessary for the effect), they give a good approximation to the velocity changes expected. The results of Nur and Simmons for saturated and dry Westerly granite are shown in Fig. 4. Nur (8) used these data to explain the changes in the V_P/V_S ratio, although Savarensky (1), whose work he referred to, stated that the stronger effect is shown by the velocities of the transverse (*S*) waves. This is in disagreement with the data of Fig. 4b and with the results reported here. Shallow saturated crustal rocks would be characterized by point *A* in Fig. 4. If dilatancy were then to occur, the fluid pore pressure would drop rapidly until the rock becomes undersaturated, the rock would strengthen, and the rock velocities would change toward point *B*. During this drop of V_P/V_S both V_P and V_S decrease, but the drop of V_P dominates because of the significantly decreased bulk modulus of the rock, which results from undersaturation. Subsequent fluid flow would then bring the rock to a saturated state at a rate dependent on dilatancy volume, permeability, and availability of fluids. When point *C* (shown in Figs. 1 and 4) is reached, the rock weakens and an earthquake occurs. The characters and amplitudes of the velocity changes between *A*, *B*, and *C* in Figs. 1 and 4 are remarkably similar.

The independence of the size of the precursory drop of ($V_P/V_S - 1$) with magnitude, found by Semenov (2) and Aggarwal *et al.* (4) and confirmed here, is easily understood. The velocity variations of this model depend mainly on the range of rock velocities between saturated and undersaturated states at low effective confining pressures, which has no relation to earthquake magnitude or volume of dilatant rock.

An implication of the results is that some of the crustal rocks between PAS and RVR, which are more than 35 km from the aftershock region of the San Fernando earthquake, were significantly dilatant before the earthquake, which had characteristic dimensions of only about 20 km. The following proposed sequence may explain this. Some part of the region near San Fernando, not necessarily the location of the earthquake hypocenter, reached its strength limit due to increasing regional tectonic strain. Dilatancy occurred (*10*) and dilatancy hardening strengthened the dilatant volume. Because stress concentrates around strength inhomogeneities, the next tectonic strain increment dilated the surrounding volume and subsequent increments continued the process over a larger and larger volume. Meanwhile, fluid flow into the volume began from all sides. In general, the fluid pore pressure first reached its saturated value where the permeability was greatest. Thus, permeability may have controlled the location of the initial rupture. Permeability may be greater along deep fracture zones, and it is significant to note that seismicity before the San Fernando earthquake

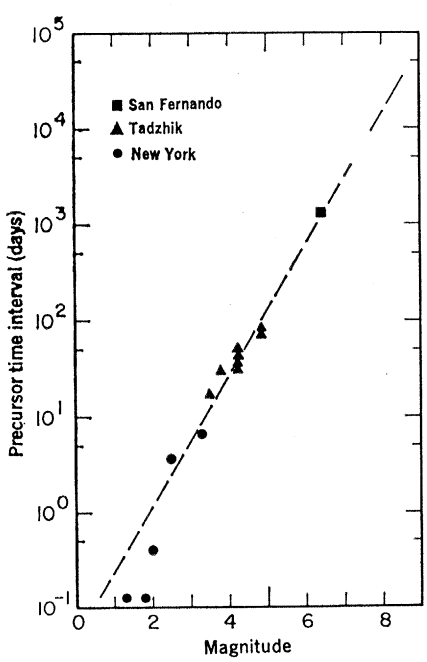

Fig. 3. The anomalous velocity precursor time interval as a function of earthquake magnitude for the 1971 San Fernando earthquake (square) and previous data from Semenov (2) (triangles) and Aggarwal *et al.* (4) (circles).

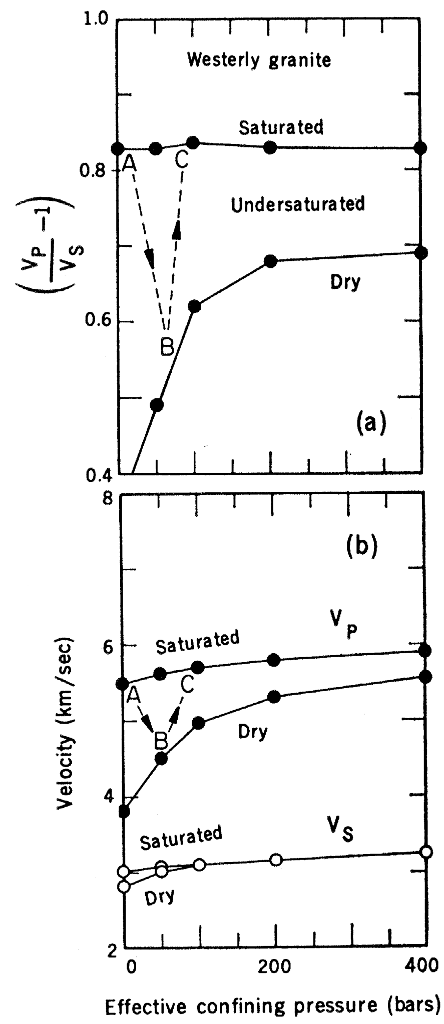

Fig. 4. (a) Velocity data from Nur and Simmons (9) reduced to the form ($V_P/V_S - 1$) for saturated and dry Westerly granite, as a function of effective confining pressure. See the text for an explanation of *A*, *B*, and *C*. (b) Velocities V_P and V_S for the same data.

outlined a seismic zone that coincides with the hypocenter of the main event and a downstep in the main fault surface (*5*). This seismic zone may have controlled the initial rupture location of the San Fernando earthquake. The extent of fracturing in the main earthquake depends on the details of the stress, strength, and pore pressures in the dilatant volume and need not be as great as the prerupture dilatant volume.

It is tempting to extend the analysis to the variations of *P*-wave velocity observed during 1961 to 1962 (Fig. 1b), a time when the above-mentioned zone through the San Fernando earthquake epicenter was active (*5*). However, this will be reserved for future work with a more complete data set.

If we can assume that the size of an earthquake is related to the amount of stored mechanical energy in crustal rocks near the epicentral area, then there should be a positive relation between dilatant volume and magnitude because dilatant rock is strained to near-rupture levels and has additional stored energy due to dilatancy. This points the way to an explanation of the observed relation between earthquake magnitude and precursor time interval (Fig. 3); it derives from the time needed for fluid flow to restore undersaturated rock in the dilatant volume to the saturated state. Thus, a longer precursor time interval implies a larger dilatant volume, which is turn leads to larger earthquakes.

The relation between magnitude (M) and anomaly time (t) from the data in Fig. 3 is

$$\log t = 0.68M - 1.31$$

where t is in days. A similar relationship was derived by Tsubokawa (*11*) on the basis of ground deformation before Japanese earthquakes. Combining his data with the present data set we obtain

$$\log t = 0.80M - 1.92$$

which predicts lead times of 13 years for a magnitude 7 and 83 years for a magnitude 8 earthquake.

The physics of the situation is clearer if we plot time against some earthquake dimension such as fault length or volume. In Fig. 5 we have plotted delay time as a function of a characteristic linear dimension. The latter is estimated from the aftershock area for the larger earthquakes and from an empirical relation between fault length and magnitude (*12*) for the earthquakes from New York State and the Soviet Union. The data are those in Fig. 3 plus data for five large earthquakes in Japan (*11*). The data are fit well by a relation involving the square root of time, which suggests that the duration of the anomaly is controlled by the flow of water into the stressed region, as proposed earlier. The constant term D in the fluid flow equation $L = Dt^{1/2}$, when L is "fault length" or square root of aftershock area and t is the time, is a function of permeability, porosity, fluid properties, the driving head, and a factor relating aftershock area or fault length to the dilated regions. There is much uncertainty in all of these parameters, but one can estimate that the required permeability is several orders of magnitude greater than that of unfractured granite.

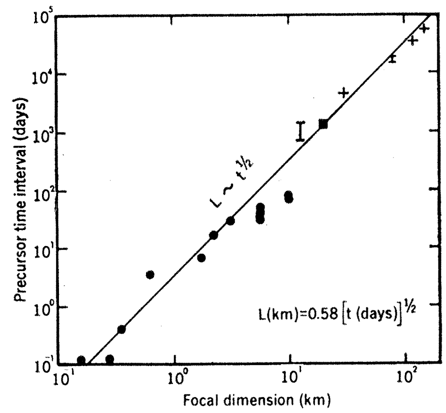

Fig. 5. Precursor time interval as a function of earthquake dimension for the data in Fig. 3 (square, San Fernando earthquake; circles, Tadzhik and New York data) plus the data of Tsubokawa (*11*) (pluses and bars). The dimension is proportional to the square root of time, which suggests a fluid flow process.

It is quite amazing that earthquakes from so many different regions fall on a single curve. The result implies that igneous crustal rocks stressed to near-failure behave in a similar fashion and that the stress-induced porosities and permeabilities are similar. However, this is probably more likely than the alternate explanation, namely, that the anomaly duration is a function of regional stresses and stress changes.

We conclude that velocity variations show significant promise as earthquake precursors. The combined evidence from the magnitudes of the velocity drops and the diffusive-like recovery behavior gives strong support to the idea that the anomaly is initiated by increasing the pore volume in a saturated rock. The process is then terminated by the gradual return to saturated conditions which precede failure, that is, a mechanism involving dilatancy, dilatancy hardening, and flow of fluid through a semipermeable medium. The observation that *P*-wave velocity variation is greater than the *S*-wave velocity variation not only confirms the dilatancy–fluid saturation theory, but has important implications for the course of future investigations. Because the time of arrival of *P* waves is much easier to measure than that of *S* waves, not only earthquakes but artificial sources such as large mine blasts can be used to monitor crustal velocities for the purpose of earthquake prediction.

This work suggests that other phenomena associated with dilatancy, such as electrical conductivity, ground tilts, changes in ground elevation (which might be of the order of tens of centimeters), and deep well levels and pressures, may also be useful in earthquake prediction. It also suggests a possible method of control, at least for shallow earthquakes, based on rapid and widespread well pumping to vary the fluid distribution in the crust so that we may choose the time of earthquake rupture.

JAMES H. WHITCOMB
JAN D. GARMANY
DON L. ANDERSON
Seismological Laboratory,
Bin 2, Arroyo Annex,
Pasadena, California 91109

References and Notes

1. E. F. Savarensky, *Tectonophysics* **6**, 17 (1968). However, there is a possible conflict between the statements and data presented relative to the V_P and V_S changes.
2. A. N. Semenov, *Izv. Acad. Sci. USSR Phys. Solid Earth* **4**, 245 (1969).
3. I. L. Nersesov, A. N. Semenov, I. G. Simbireva, in *The Physical Basis of Foreshocks* (Nauka, Moscow, 1969).
4. Y. P. Aggarwal, L. R. Sykes, J. Armbruster, M. L. Sbar, *EOS Trans. Amer. Geophys. Union* **53**, 1041 (1972); *Nature* **241**, 101 (1973).
5. J. H. Whitcomb, C. A. Allen, J. D. Garmany, J. A. Hileman, *Rev. Geophys.*, in press.
6. F. C. Frank, *ibid.* **3**, 485 (1965).
7. W. F. Brace and R. J. Martin III, *Int. J. Rock Mech. Min. Sci.* **5**, 415 (1968).
8. A. Nur, *Bull. Seismol. Soc. Amer.* **62**, 1217 (1972); *EOS Trans. Amer. Geophys. Union* **53**, 1115 (1972).
9. ——— and G. Simmons, *Earth Planet. Sci. Lett.* **7**, 183 (1969).
10. W. F. Brace, B. W. Paulding, Jr., C. H. Scholz, *J. Geophys. Res.* **71**, 3939 (1966).
11. I. Tsubokawa, *J. Geodet. Soc. Jap.* **15**, 75 (1969) (in Japanese).
12. M. Wyss and J. N. Brune, *J. Geophys. Res.* **73**, 4681 (1968).
13. We thank Y. P. Aggarwal, L. R. Sykes, J. Armbruster, and M. L. Sbar for a preprint of their paper. H. Kanamori made many useful contributions and reviewed the manuscript. Supported by U.S. Geological Survey contract 14-08-0001-12714 and by NASA contract 49-615-95650-0-3910 to the Jet Propulsion Laboratory. Contribution No. 2284, Division of Geological and Planetary Sciences, California Institute of Technology.

29 December 1972; revised 27 March 1973